MCB
Journals.ASM.org

Poly(A) Tail-Mediated Gene Regulation by Opposing Roles of Nab2 and Pab2 Nuclear Poly(A)-Binding Proteins in Pre-mRNA Decay

Valérie Grenier St-Sauveur,[a] Sharon Soucek,[b] Anita H. Corbett,[b] François Bachand[a]

RNA Group, Université de Sherbrooke, Department of Biochemistry, Québec, Canada[a]; Department of Biochemistry, Emory University School of Medicine, Atlanta, Georgia, USA[b]

The 3′ end of most eukaryotic transcripts is decorated by poly(A)-binding proteins (PABPs), which influence the fate of mRNAs throughout gene expression. However, despite the fact that multiple PABPs coexist in the nuclei of most eukaryotes, how functional interplay between these nuclear PABPs controls gene expression remains unclear. By characterizing the ortholog of the Nab2/ZC3H14 zinc finger PABP in *Schizosaccharomyces pombe*, we show here that the two major fission yeast nuclear PABPs, Pab2 and Nab2, have opposing roles in posttranscriptional gene regulation. Notably, we find that Nab2 functions in gene-specific regulation in a manner opposite to that of Pab2. By studying the ribosomal-protein-coding gene *rpl30-2*, which is negatively regulated by Pab2 via a nuclear pre-mRNA decay pathway that depends on the nuclear exosome subunit Rrp6, we show that Nab2 promotes *rpl30-2* expression by acting at the level of the unspliced pre-mRNA. Our data support a model in which Nab2 impedes Pab2/Rrp6-mediated decay by competing with Pab2 for polyadenylated transcripts in the nucleus. The opposing roles of Pab2 and Nab2 reveal that interplay between nuclear PABPs can influence gene regulation.

Production of mRNA in eukaryotic cells is a multistep procedure that involves extensive RNA-processing events, such as 5′-end capping, removal of introns by RNA splicing, 3′-end cleavage, and polyadenylation. Polyadenylation has received considerable interest in the past few years, as recent evidence has revealed that polyadenylation can promote RNA turnover in eukaryotic cells (1–5), contrary to the general view that poly(A) tails only contribute positively to gene expression. The extent to which polyadenylation contributes to RNA turnover and the mechanisms that specify this specialized RNA decay pathway remain poorly understood, however.

The fundamental role of RNA polyadenylation in gene expression is conferred by the activity of poly(A)-binding proteins (PABPs) that bind to the 3′ poly(A) tail of eukaryotic mRNAs. Two evolutionarily conserved RNA recognition motif (RRM)-containing PABPs bind the poly(A) tract of mRNAs in most eukaryotic cells: PABPC1 in the cytoplasm and PABPN1 in the nucleus (6). Biochemical studies on PABPN1 led to a model in which the protein promotes efficient polyadenylation during mRNA synthesis (7). Although a role for PABPN1 in modulating poly(A) tail length is supported by studies in primary mouse myoblasts (8), studies in human cell lines have recently revealed novel functions for PABPN1. One study demonstrated that PABPN1 modulates the use of alternative polyadenylation sites by occluding access to weak polyadenylation signals for a select group of human genes (9, 10). In addition, a recent genome-wide study that addressed the global impact of PABPN1 deficiency on human gene expression uncovered a role for PABPN1 in the negative regulation of long noncoding RNAs (lncRNAs) (11). Interestingly, a 3′ poly(A) tail is a prerequisite for PABPN1 to promote lncRNA turnover (11), consistent with a mechanism of polyadenylation-mediated degradation. The identification of a role for PABPN1 in polyadenylation-dependent RNA decay echoes findings that originate from studies of the fission yeast PABPN1 homolog, Pab2. Accordingly, Pab2 promotes nuclear turnover of specific meiotic transcripts during the mitotic cell cycle (3) by physically associating with the exosome (2), a barrel-like complex that contains 10 core subunits, including the 3′-5′ exonuclease Dis3/Rrp44 and an additional 3′-5′ exonuclease, Rrp6, in the nucleus (12, 13). Pab2 also functions in a nuclear pre-mRNA decay pathway that controls the expression of specific intron-containing genes (14). In the case of the intron-containing ribosomal-protein gene *rpl30-2*, its paralog, Rpl30-1, acts as a negative regulator by interfering with *rpl30-2* splicing. Splicing inhibition of *rpl30-2* by Rpl30-1 sensitizes the unspliced *rpl30-2* pre-mRNA to nuclear decay via Pab2 and the exosome subunit Rrp6 (14). The equilibrium between Pab2/Rrp6-mediated pre-mRNA decay and RNA splicing thus provides an important mechanism to maintain balanced levels of paralogous ribosomal proteins in yeast.

In contrast to PABPN1 and Pab2, which bind to poly(A) RNA using a single and conserved RRM (15, 16), a different class of evolutionarily conserved nuclear PABPs that recognize poly(A) RNA via Cys-Cys-Cys-His (CCCH) zinc finger (ZnF) motifs has also been described (17, 18). *Saccharomyces cerevisiae* Nab2 is the CCCH zinc finger PABP that has been most extensively studied to date. *nab2* encodes an essential nuclear protein that harbors seven CCCH ZnF motifs, of which ZnF5 to -7 are necessary and sufficient for high-affinity binding to poly(A) RNA (19, 20). Functionally, Nab2 has been implicated in two distinct steps of budding yeast gene expression: mRNA export and poly(A) tail length control (21). Nab2 contributes to the RNA export process by recruiting mRNA export factors (22) and by interacting with nuclear pore-associated proteins (23), interactions that involve a Pro-

Received 12 July 2013 Returned for modification 21 August 2013
Accepted 19 September 2013
Published ahead of print 30 September 2013
Address correspondence to François Bachand, f.bachand@usherbrooke.ca.
Supplemental material for this article may be found at http://dx.doi.org/10.1128/MCB.00887-13.

doi:10.1128/MCB.00887-13

Trp-Iso (PWI)-like fold located in the amino-terminal region of Nab2 (24). RNA from *nab2* mutant cells also displays longer poly(A) tails (25). The findings that Nab2 mutants with substitutions in ZnF5 to -7 are impaired in poly(A) binding *in vitro* and result in hyperadenylated RNA *in vivo* suggested that the function of Nab2 in polyadenylation control requires poly(A)-bound Nab2 (20). As yet, however, the identities of the hyperadenylated transcripts in Nab2-deficient cells remain unknown. Interestingly, although Nab2 appears to associate with the bulk of the *S. cerevisiae* mRNA transcriptome (26), cells deficient for Nab2 mainly affect the expression of intron-containing genes (27). Specifically, *nab2*-deficient cells accumulate unspliced pre-mRNAs but not spliced mRNAs (27). Although the exact mechanism by which Nab2 controls unspliced pre-mRNA levels remains to be determined, a physical interaction detected between Nab2 and the exosome subunit Rrp6 has led to a model in which Nab2 functions in the quality control of gene expression by promoting Rrp6-mediated decay in the nucleus (27).

Nab2 orthologs have also been identified in *Drosophila*, *Caenorhabditis elegans*, and humans, referred to as dNab2, Sut2, and ZC3H14, respectively (28). In *Drosophila*, *dnab2* mutant flies exhibit defects in poly(A) tail length control but do not appear to be affected in poly(A) RNA export (29). In *C. elegans*, Sut2 was identified as a suppressor of Tau pathology, but molecular functions have not been reported (30). In humans, nuclear and cytoplasmic isoforms are expressed from the *ZC3H14* gene (18), but the functions of these isoforms remain to be determined. Interestingly, loss of the nuclear isoform leads to intellectual disability (28, 29), highlighting the importance of defining the function of this class of nuclear PABP.

How different PABPs coexist in the eukaryotic nucleus and whether there is functional interplay between nuclear PABPs, such as between Nab2/ZC3H14 and Pab2/PABPN1, remain elusive. In this study, we characterize the fission yeast ortholog of human ZC3H14/Nab2 and provide evidence that Nab2 and Pab2 have opposing roles in fission yeast gene regulation. By studying the Pab2-regulated gene *rpl30-2*, we show that Nab2 functions as a positive regulator of *rpl30-2* expression, in contrast to Pab2. We also find that Nab2 preferentially binds to the *rpl30-2* unspliced pre-mRNA relative to the spliced transcript. Consistent with this finding, the ability of Nab2 to promote *rpl30-2* expression requires the *rpl30-2* intron. Our data support a model in which Nab2 impedes Pab2/Rrp6-mediated degradation of unspliced *rpl30-2* pre-mRNA in the nucleus by competing with Pab2 for access to the poly(A) tail.

MATERIALS AND METHODS

Strains and media. All of the *Schizosaccharomyces pombe* strains used in this study are listed in Table S1 in the supplemental material. Cells were grown at 30°C in yeast extract medium with supplements (YES) or Edinburgh minimum medium (EMM) containing appropriate supplements. *prp1-4* and *prp2-1* mutants were grown at the permissive temperature of 25°C and shifted to the nonpermissive temperature of 37°C for the indicated times. Conditional expression of Nab2 was achieved using the *nmt1* promoter, which is repressed in the presence of 15 μM thiamine. To allow Nab2 expression, cells were washed twice and then grown without thiamine for 15 h. Gene disruptions were done using either the PCR-mediated gene-targeting method (31) or a two-step approach modified from the first method. All gene deletions were confirmed by colony PCR from genomic DNA and reverse transcription (RT)-PCR.

Structural homology modeling. Homology models of *S. pombe* Nab2 (SPAC14C4.06c) were constructed using Swiss-Model (version 8.05; [32]), starting with the known *S. cerevisiae* Nab2 crystal structure (Protein Data Bank [PDB] entry 2V75 [24]). The model was energy minimized in CNS 1.2 to remove any steric strain introduced during modeling (33). The model was visualized, and protein backbone torsion angles (phi and psi) were verified in Coot (34).

DNA constructs. All of the DNA constructs used in this study are listed in Table S2 in the supplemental material. The glutathione *S*-transferase (GST)–Nab2 expression construct was prepared by inserting the *S. pombe nab2* cDNA into pGEX-5X-3 using BamHI and XhoI restriction sites, creating pFB692. To express the wild-type version of Nab2 in the *nab2*Δ strain, the *S. pombe nab2* gene was amplified using genomic DNA with additional sequences corresponding to the promoter and the terminator of the *nab2* gene. This PCR product was cloned into pBPade6 (35) using PstI and NotI restriction sites to create the plasmid pFB815. Site-directed mutagenesis was performed using pFB815 to replace the first cysteine of each CCCH zinc finger motif with an alanine, generating plasmid pFB834. pAde6-derived constructs were linearized with BamHI and transformed in the *nab2*Δ strain for single integration at the *ade6* chromosomal locus. The expression of the various *S. pombe nab2* alleles was confirmed by RT-PCR. To express green fluorescent protein (GFP)-Nab2 under the control of the *nmt1* promoter, the *S. pombe nab2* cDNA was cloned into pREP42 EGFP-N (36) using NdeI and BamHI sites to generate pFB720. All of the aforementioned plasmid constructs were confirmed by DNA sequencing.

Microscopy. Nab2-GFP was visualized by direct live microscopy as previously described (37). Briefly, cells were grown in EMM, immobilized on concanavalin A-precoated slides, and washed extensively with EMM to remove unfixed cells. Nuclear DNA was stained using Hoechst 33342. GFP signals were visualized using a 62HE triple filter (Carl Zeiss, Canada) on an Oberver.Z1 (Carl Zeiss, Canada) equipped with a Cascade II camera (Carl Zeiss, Canada). Cellular autofluorescence background signals were removed using Axio Vision 4.7 software (Carl Zeiss, Canada).

Recombinant protein expression, RNA electrophoretic mobility shift assays, and *in vitro* degradation assays. GST, GST-Pab2, GST-Nab2, and GST-Nab2 with ZnF substitutions were expressed and purified as described previously (38) with the exception that 10 μM $ZnCl_2$ was systematically added throughout the purification to allow proper Nab2 folding. All proteins were stored at 4°C, and binding assays were performed within 48 h. Expression and purification of recombinant *S. pombe* Rrp6-Flag were described previously (2).

RNA gel shift assays were performed by incubating control GST alone or GST fusion proteins in binding buffer (20 mM Tris-HCl, pH 7.4, 50 mM NaCl, 2 μM $ZnCl_2$, 2% glycerol) in the presence of a Cy3-labeled 25-nucleotide (nt)-long poly(A) RNA oligonucleotide (IDT) for 30 min at room temperature. Binding reaction mixtures were loaded onto a native 5% polyacrylamide gel (PAGE) in 0.3× Tris-borate-EDTA (TBE). Free Cy3-poly(A) RNA and bound complexes were visualized using a Typhoon Trio instrument (GE Healthcare). For protein displacement experiments, GST-Pab2 and GST-Nab2 (5 pmol) binding reaction mixtures were incubated for 15 min at room temperature and then supplemented with increasing amounts of GST-Nab2 (500 fmol [0.1×], 1 pmol [0.2×], 5 pmol [1×], and 10 pmol [2×]) or GST-Pab2 (5 pmol [1×], 10 pmol [2×], 20 pmol [4×], and 40 pmol [8×]), respectively, for an additional 15 min before PAGE analysis.

In vitro RNA degradation assays were performed with a constant amount of Cy3-poly(A) RNA (20 nM) but with increasing amounts of Rrp6 enzyme in a solution containing 10 mM Tris-Cl, pH 8.0, 50 mM KCl, 7.1 mM MgCl, and 75 μM MnCl. Degradation assays were allowed to proceed for 1 h at 25°C, after which they were quenched by the addition of RNA loading buffer and separated by denaturing gel electrophoresis in 20% urea-acrylamide gels and visualized using a Typhoon Trio imager. To test the effect of Nab2 on Rrp6-mediated degradation, 7.5 pmol of wild-type and C184A versions of GST-Nab2 (the amount required for wild-

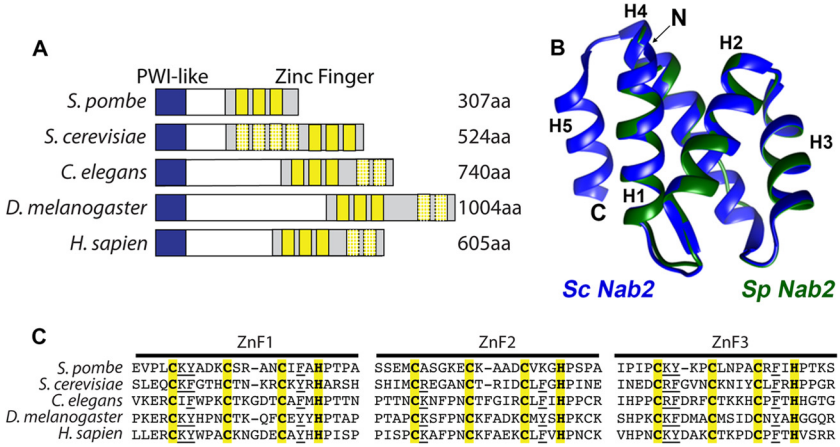

FIG 1 SPAC14C4.06c is a conserved CCCH zinc finger protein. (A) Domain alignment of *S. pombe* SPAC14C4.06c, *S. cerevisiae* Nab2, *C. elegans* Sut2, *Drosophila melanogaster* dNab2, and *Homo sapiens* ZC3H14. The N-terminal domain contains a PWI-like motif (blue), and the C-terminal domain consists of a series of tandem zinc fingers (yellow). The zinc fingers most similar to *S. pombe* ZnF1 to -3 are shown in solid yellow boxes and are used in the alignment shown in panel C. The crosshatched yellow boxes indicate additional zinc fingers present in other species. (B) Homology model of the N-terminal domain (amino acids 1 to 79) of *S. pombe* SPAC14C4.06c (green) overlaid with the N-terminal domain (amino acids 1 to 93) of *S. cerevisiae* Nab2 (blue). Homology modeling was carried out as described in Materials and Methods. The molecular images were generated using PyMol. (C) Alignment of the three C-terminal zinc finger motifs of *S. pombe* SPAC14C4.06c with zinc fingers of Nab2 orthologs: *S. cerevisiae* ZnF5 to -7 and *C. elegans*, *Drosophila*, and human ZnF1 to -3. These zinc fingers share both spacing and conservation of key cysteine and histidine residues (yellow) required for optimal RNA binding (indicated by underlining).

type Nab2 to shift 100% of the RNA probe) were preincubated for 15 min with poly(A) RNA before the addition of increasing amounts of Rrp6.

Affinity purification coupled to mass spectrometry analysis. Nab2-ProA was affinity purified using a previously described method (39). Briefly, cells were harvested at mid-log phase and frozen in liquid nitrogen. The cell pellets were washed once with water and once in resuspension buffer (1.2% polyvinylpyrrolidone, 20 mM HEPES, pH 7.4, 1 mM dithiothreitol [DTT], and protein inhibitors) before lysis by cryogenic grinding. Extraction buffer (100 mM HEPES, pH 7.4, 150 mM NaCl, 0.5% Triton, 1 mM DTT, 1.5 mM $MgCl_2$, 20 ng pepstatin, 900 ng phenylmethylsulfonyl fluoride [PMSF], 0.1% ethanol) was then added to the ground cells and homogenized using a Polytron (Kinematica). Cell lysates were centrifuged for 10 min at 3,500 rpm (4°C) and incubated with prewashed antibody-conjugated magnetic beads for 30 min (4°C). The beads were washed three times with extraction buffer and five times with wash buffer (0.1 M ammonium acetate [NH_4OAc], 0.1 mM $MgCl_2$). Proteins were eluted twice in elution buffer (0.5 M NH_4OAc, 0.5 mM EDTA) for 20 min at room temperature and vacuum dried. Protein samples were resuspended in loading buffer before being reduced in 10 mM DTT and alkylated in 50 mM iodoacetamide prior to SDS-PAGE (4 to 12% Bis-Tris Novex minigel; Invitrogen) separation. Following visualization by colloidal Coomassie staining, entire gel lanes were excised and cut into eight equal-size pieces that were subjected to in-gel digestion using trypsin. Tryptic peptides were separated using an Ultimate U3000 (Dionex Corporation) nanoflow liquid chromatography (LC) system coupled to an LTQOrbiTrapVelosmassspectrometer.Theresultingtandemmassspectrometry (MS-MS) spectra were searched against the PomBase protein data set using MASCOT for peptide identifications.

RNA analyses. Total RNA was extracted using the hot-acid phenol method. For Northern blot analyses, total RNA was resolved on agarose-formaldehyde or polyacrylamide-urea gels, transferred onto nylon membranes, and probed using ^{32}P-labeled gene-specific probes. Bulk poly(A) tail length analysis was done as described previously (38). RNase H cleavage assays (2) and real-time RT-PCR (3) analyses were performed as previously described. To measure *rpl30-2* mRNA stability, transcription was blocked with 300 μg/ml 1,10-phenanthroline as described previously (40), followed by RNA extraction from cells harvested at the indicated time points.

ChIP assays. Chromatin immunoprecipitation (ChIP) assays were carried out as previously described (41).

RESULTS

The *S. cerevisiae* and human PABPs, Nab2 and ZC3H14, respectively, are part of a novel class of conserved PABPs that recognize poly(A) RNA via tandem CCCH zinc finger motifs (17). To search for Nab2/ZC3H14 orthologs in the fission yeast *S. pombe*, we performed BLAST analyses to identify an ortholog containing CCCH zinc fingers with spacing similar ($CX_5CX_{4-6}CX_3H$) to those found in *S. cerevisiae* Nab2 and human ZC3H14 (17). Our sequence analyses identified an *S. pombe* protein, SPAC14C4.06c, with tandem CCCH zinc finger motifs that share similar domain structures with Nab2 proteins from *S. cerevisiae*, *C. elegans*, *Drosophila*, and humans (Fig. 1A). Comparison of the overall sequence similarity of SPAC14C4.06c with Nab2 orthologs revealed a high level of similarity between the N-terminal and C-terminal domains, with less sequence conservation in the central region (see Fig. S1 in the supplemental material). Importantly, *in silico* structure simulations of the N-terminal region of *S. pombe* SPAC14C4.06c (Fig. 1B) nicely matched the resolved structure of the PWI-like domain of *S. cerevisiae* Nab2 (24). As illustrated in Fig. 1A and C, *S. pombe* SPAC14C4.06c contains three zinc finger domains, whereas *S. cerevisiae* Nab2 and human ZC3H14 contain seven and five zinc fingers, respectively. Only three zinc fingers (ZnF5 to -7) within *S. cerevisiae* Nab2 are required for high-affinity binding to poly(A) RNA (20) and also to fold into a stable poly(A) RNA binding module (19). Thus, *S. pombe* SPAC14C4.06c, which contains only three CCCH zinc fingers, may represent a minimal version of this protein family. Indeed, comparison of the amino acid sequences within the CCCH zinc fingers of *S. pombe* SPAC14C4.06c to sequences in the zinc finger motifs documented to mediate RNA binding in *S. cerevisiae* Nab2 shows conservation of key intervening residues required to mediate RNA binding, in addition to the structural Cys and His residues (Fig. 1C). On the basis of the aforementioned sequence and structural similarities, we named *S. pombe* SPAC14C4.06c Nab2.

Fission yeast Nab2 is a nonessential nuclear poly(A)-binding protein. We constructed a diploid *S. pombe* strain in which one of

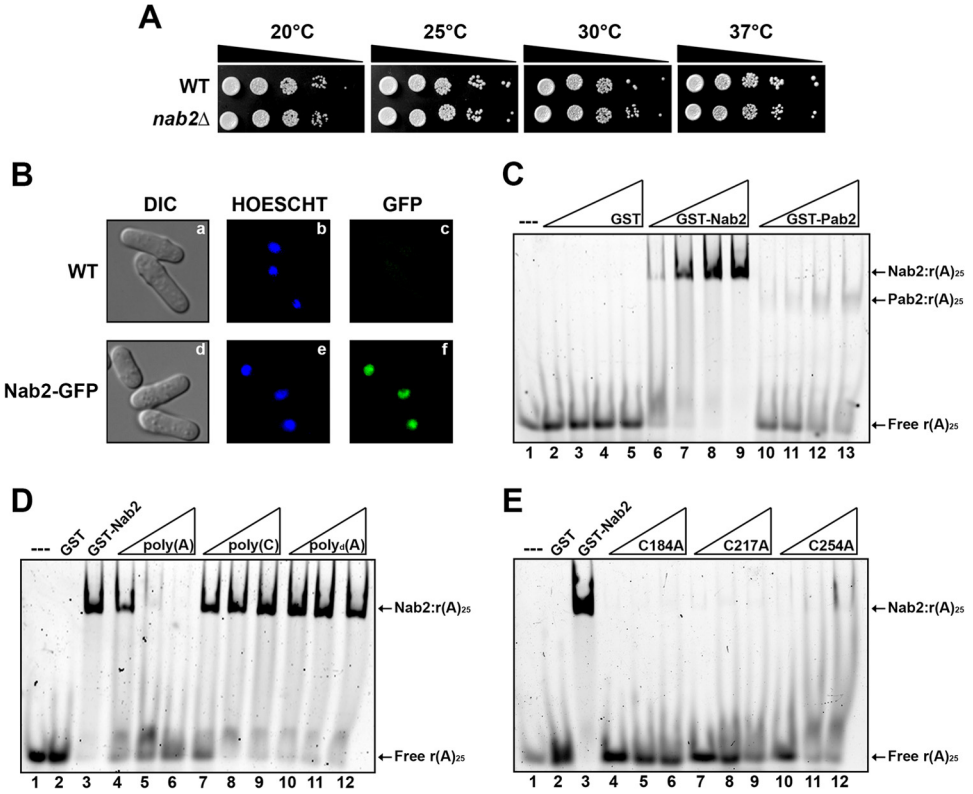

FIG 2 *S. pombe* Nab2 is a nonessential nuclear poly(A)-binding protein. (A) Tenfold serial dilution of wild-type (WT) and *nab2*Δ strains. (B) Visual analysis of control (a to c) and GFP-Nab2 (d to f) living cells. DIC, differential interference contrast. (C) Equal amounts of GST (lanes 2 to 5), GST-Nab2 (lanes 6 to 9), and GST-Pab2 (lanes 10 to 13) were incubated with a Cy3-poly(A) RNA [$r(A)_{25}$], and RNA-protein complexes were analyzed on nondenaturing polyacrylamide gels. The arrows point to the positions of free $r(A)_{25}$, as well as Pab2-$r(A)_{25}$ and Nab2-$r(A)_{25}$ complexes. (D) Equal amounts of GST-Nab2 were incubated with Cy3-$r(A)_{25}$ in the presence of increasing concentrations of poly(A) (lanes 4 to 6), poly(C) (lanes 7 to 9), and poly(dA) (lanes 10 to 12) or without any competing nucleic acid (lane 3). (E) An equal amount of Cy3-$r(A)_{25}$ was incubated with GST (lane 2), wild-type GST-Nab2 (lane 3), and increasing concentrations of GST-Nab2 C184A (lanes 4 to 6), GST-Nab2 C217A (lanes 7 to 9), and GST-Nab2 C254A (lanes 10 to 12) and analyzed as described for panel C.

the two alleles of *nab2* was disrupted to assess whether *nab2* is essential for viability. Germination of the spores after meiosis resulted in a 2:2 segregation ratio of Geneticin resistance, indicating that *nab2*-null cells are viable in *S. pombe*. Examination of cell growth revealed that *nab2*-null cells grow comparably to wild-type cells at different temperatures (Fig. 2A). We next monitored Nab2 localization in live cells using a GFP fusion. GFP-Nab2 localized to cell nuclei and was excluded from the cytoplasm at steady state (Fig. 2B, panels d to f). Thus, in contrast to *S. cerevisiae* and *Drosophila*, nuclear Nab2 is not essential for mitotic growth in *S. pombe*.

S. cerevisiae Nab2 specifically binds synthetic adenylate chains *in vitro* (17). To test whether *S. pombe* Nab2 shares the same function, we expressed the full-length *S. pombe* Nab2 protein in *Escherichia coli* as a GST fusion and examined the binding to poly(A) RNA in gel shift assays using a Cy3-poly$(A)_{25}$ RNA [Cy3-$r(A)_{25}$] oligonucleotide. GST-Nab2 robustly bound the poly(A) RNA oligonucleotide (Fig. 2C, lanes 6 to 9), whereas GST alone did not (Fig. 2C, lanes 2 to 5). As a positive control, the other fission yeast nuclear poly(A)-binding protein, Pab2 (38), also bound to the Cy3-$r(A)_{25}$ (Fig. 2C, lanes 10 to 13). Binding of Nab2 was specific for poly(A) RNA, as neither poly(C) RNA nor single-stranded poly(dA) could compete for binding between GST-Nab2 and Cy3-$r(A)_{25}$ (Fig. 2D, lanes 7 to 12); in contrast, unlabeled poly(A) RNA efficiently competed for binding (lanes 4 to 6). We next addressed the importance of the zinc finger motifs of *S. pombe* Nab2 in binding to poly(A) RNA by generating variants of Nab2 in which the first cysteine of each CCCH zinc finger (C184, C217, and C254) was replaced by an alanine residue. Purification of GST-Nab2 C184A, GST-Nab2 C217A, and GST-Nab2 C254A yielded levels of recombinant protein similar to those of wild-type GST-Nab2 (see Fig. S2 in the supplemental material). Notably, no detectable Nab2-$r(A)_{25}$ complex was observed for the Nab2 C184 and Nab2 C217A variants (Fig. 2E, lanes 4 to 6 and 7 to 9, respectively), whereas wild-type GST-Nab2 bound strongly to poly(A) RNA (lane 3). Nab2 C254A showed smearing of the labeled poly(A) RNA probe in the gel shift assay (Fig. 2E, lanes 10 to 12), which likely reflects transient and/or unstable binding. These results indicate that *S. pombe* Nab2 can specifically bind to poly(A) RNA and that the zinc finger motifs within Nab2 are important to mediate stable binding to poly(A) RNA.

Nab2 is not required for general control of mRNA polyadenylation and does not associate with the mRNA 3′-end processing machinery. In *S. cerevisiae*, cellular depletion of functional Nab2 causes RNA hyperadenylation (25). We therefore examined whether Nab2 is similarly involved in the regulation of poly(A) tail synthesis in fission yeast. Poly(A) tail distribution was analyzed by 3′-end labeling of total RNA prepared from wild-type and *nab2*Δ strains, followed by RNase digestion, leaving the poly(A) chains intact. Comparison between RNA prepared from wild-type and

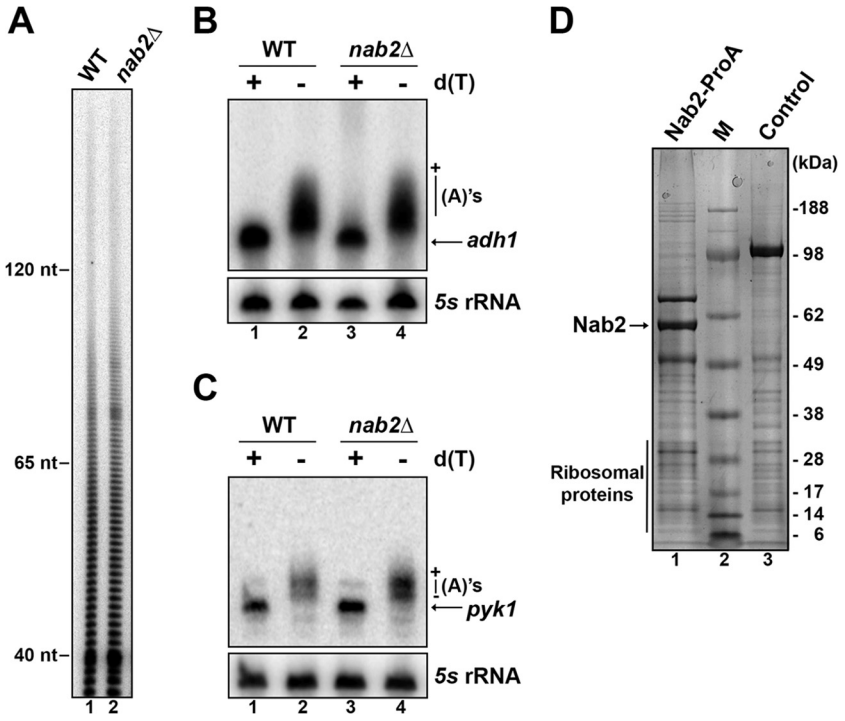

FIG 3 *S. pombe* Nab2 is not required for mRNA poly(A) tail length control. (A) Poly(A) tail length was analyzed by 3′-end labeling of total RNA extracted from the indicated strains. Following RNase degradation of non-poly(A) sequences, the poly(A) tails were separated by electrophoresis through a 15% polyacrylamide-8 M urea gel. The positions of 3′-end-labeled DNA fragments are indicated on the left. (B and C) Total RNA prepared from wild-type (lanes 1 and 2) and *nab2*Δ (lanes 3 and 4) cells was treated with RNase H in the presence of DNA oligonucleotides complementary to *adh1* (B) and *pyk1* (C) mRNAs. RNase H reactions were performed in the presence (+) or absence (−) of oligo(dT). "(A)'s" represents poly(A) tail heterogeneity. The 5S rRNA was used as a loading control. (D) Coomassie blue staining analysis of proteins copurified with Nab2-ProA (lane 1) and a control ProA fusion (lane 3). M, molecular mass markers.

*nab2*Δ strains did not reveal a significant impact on bulk poly(A) tail distribution between the two samples (Fig. 3A). We also examined the polyadenylation status of specific mRNAs by treatment with RNase H. RNase H treatment in the presence of a DNA oligonucleotide complementary to a region located in the 3′ untranslated region (UTR) of an mRNA will release heterogeneous 3′ fragments as a consequence of different poly(A) tail lengths. The addition of oligo(dT) to the RNase H reaction mixture causes this heterogeneous population of 3′ fragments to collapse into discrete products, indicating the positions of cleavage sites. As can be seen for the *adh1* and *pyk1* mRNAs, poly(A) tail lengths and cleavage site decisions were similar between wild-type and *nab2*Δ cells (Fig. 3B and C, compare lanes 3 and 4 to 1 and 2). From these results, we conclude that mRNA polyadenylation occurs normally in *S. pombe* cells with *nab2* deleted.

Given the absence of change in the polyadenylation status of the *nab2*Δ mutant, we decided to identify Nab2-associated proteins to obtain further insights into the functional role of *S. pombe* Nab2. We used a strain in which a Nab2-protein A fusion (Nab2-ProA) was expressed from its endogenous chromosomal locus using the *nab2* promoter. To control for specific interactions, we compared results obtained for Nab2-ProA to a control cytosolic RNA-binding protein, Snd1-ProA. Following affinity purification optimized to preserve the integrity of cellular ribonucleoprotein complexes (39), the eluted proteins were separated by SDS-PAGE (Fig. 3D) and analyzed by LC–MS-MS. The purification of Nab2-ProA resulted in the identification of 768 proteins (see Table S3 in the supplemental material). Interestingly, the majority of the known pre-mRNA 3′-end processing factors were absent from the Nab2 purification, consistent with the observation that mRNAs produced in *nab2*Δ cells are cleaved and polyadenylated properly. We next used computer algorithms (42) to distinguish functional protein classes within the top 10% (77 proteins) of the proteins that were identified in the Nab2 purification but that were absent or barely detectable in the Snd1-ProA control purification. The analysis identified a significant number of proteins involved in RNA splicing in the set of proteins copurified with Nab2 (Table 1). Proteins associated with the U4/U6 × U5 tri-snRNP complex ($P = 1.6e{-}12$), the U1 snRNP ($P = 5.5e{-}8$), the U2 snRNP ($P = 1.5e{-}6$), and the spliceosomal complex ($P = 2.4e{-}28$) were recovered in the Nab2 purification. Overall, of the 77 proteins that ranked in the top 10% of the Nab2 purification, 31 (40%) have been previously shown or predicted to be involved in RNA splicing (Table 1). Interestingly, proteins involved in snoRNA binding/processing and RNA decay were also enriched in the Nab2 purification (Table 1). In conclusion, our affinity purification approach suggests that Nab2 is associated, directly or via RNA, with factors involved in processing events that include RNA splicing, snoRNA metabolism, and RNA decay.

Opposing roles for Nab2 and Pab2 in gene regulation. The identification of proteins involved in RNA splicing, snoRNA processing, and RNA degradation in the Nab2 affinity purification revealed a striking parallel with functions attributed to the other fission yeast nuclear PABP, Pab2. Pab2 was shown to function in the maturation of polyadenylated snoRNA precursors into mature snoRNAs (2, 41), as well as in the degradation of a specific set

TABLE 1 Proteins enriched in Nab2-ProA purification

Protein name	Systematic name	Mass (kDa)	Intensity[a]	% coverage[b]	Peptide no.[c]
RNA splicing					
Prp19	SPAC29A4.08c	54.2	92,000,000	54.1	23
Spp42	SPAC4F8.12c	274.6	68,700,000	56.8	120
Cwf10	SPBC215.12	11.2	32,100,000	59.4	55
Prp31	SPBC119.13c	57.7	30,100,000	8.7	3
Cwf11	SPBC646.02	148.4	27,500,000	53.6	56
Cwf3	SPBC211.02c	92.6	22,500,000	65.1	53
Prp10	SPAC27F1.09c	135.2	21,800,000	52.6	48
Brr2	SPAC9.03c	248.8	21,100,000	43.1	77
Cwf4	SPBC31F10.11c	80.8	19,000,000	45.8	30
Nog1	SPBC651.01c	72.8	19,000,000	48.8	31
Prp12	SPAPJ698.03c	134.9	14,600,000	43.4	45
Prp17	SPBC6B1.10	63.1	14,500,000	43.9	24
Smd2	SPAC2C4.03c	13.1	13,700,000	55.7	6
Cdc5	SPAC644.12	86.8	12,055,000	53.6	37
Cwf22	SPBC13E7.01	102.7	9,650,000	40.4	35
Prp45	SPCC188.11	62.7	9,010,000	42.2	17
Spf38	SPBC1289.11	37.4	8,910,000	73.5	19
Smd1	SPAC27D7.07c	13.1	8,340,000	57.3	5
Prp43	SPBC16H5.10c	83.8	7,860,000	32.4	20
Smb1	SPAC26A3.08	15.5	7,620,000	59.2	8
Smd3	SPBC19C2.14	11.0	7,410,000	60.8	5
Prp5	SPBP22H7.07	52.4	7,030,000	59.2	20
Lea1	SPBC1861.08c	27.2	6,690,000	77.0	14
Sap114	SPAC22A12.09c	54.4	6,560,000	37.6	13
Smf1	SPBC3E7.14	8.7	6,040,000	88.5	6
Sap145	SPAC22F8.10c	69.2	6,020,000	24.1	13
Usp105	SPBC4B4.09	71.3	5,850,000	39.1	27
Cwf15	SPBC337.06c	30.4	5,610,000	47.5	13
snoRNA processing					
Cbf5	SPAC29A4.04c	53.1	64,500,000	60.3	25
Fib1	SPBC2D10.10c	32.0	44,500,000	69.3	20
Nop56	SPBC646.10c	55.4	33,000,000	62.4	23
Rrp5	SPCC1183.07	187.5	31,700,000	50.8	75
Nop58	SPAC23G3.06	55.8	24,500,000	56.3	24
Gar1	SPBC20F10.01	20.1	13,900,000	46.4	6
Nhp2	SPAC1782.10c	17.2	12,100,000	53.6	6
Nrap	SPBC776.08c	126.1	10,577,000	42.4	42
Snu13	SPAC607.03	13.5	7,010,000	72.8	5
Nop2	SPBP8B7.20c	68.9	5,620,000	33.2	18
RNA decay					
Upf1	SPAC16C9.06c	104.5	63,500,000	74.4	64
SPAC17H9.02	SPAC17H9.02	118.5	14,400,000	45.5	41
Mmi1	SPCC736.12c	54.5	46,600,000	63.3	27
Mtr4	SPAC6F12.16c	126.2	6,140,000	37.2	35

[a] Relative abundance (peptide intensity).
[b] Sequence coverage.
[c] Number of unique peptides.

of unspliced pre-mRNAs in the nucleus (14). To begin to characterize the functional relationship between Pab2 and Nab2, double-mutant cells were generated. Growth of the *nab2*Δ *pab2*Δ double-mutant strain was impaired at all temperatures tested compared to either single mutant (Fig. 4A). The genetic interaction between *nab2* and *pab2* was also supported by RNA analyses: deletion of *nab2* from the *pab2*Δ strain exacerbated the previously described (38) hyperadenylation phenotype of the *pab2*Δ single mutant (Fig. 4B, compare lanes 3 and 4). However, the increased level of hyperadenylated RNAs in the *nab2*Δ *pab2*Δ double-mutant strain relative to the *pab2*Δ single mutant did not appear to affect mRNAs in general, as demonstrated by RNase H cleavage assays for the *adh1* and *pyk1* transcripts, which showed similar poly(A) tail lengths among wild-type, *nab2*Δ, *pab2*Δ, and *nab2*Δ *pab2*Δ strains (Fig. 4C and D). This observation is consistent with results indicating that Pab2 is not a general factor required for mRNA polyadenylation (2) and suggests that the increased level of hyperadenylated RNAs in the double mutant may specifically affect transcripts targeted by Pab2-dependent regulation.

To test the hypothesis that Nab2 may target Pab2-regulated transcripts, we first examined the expression of two independent snoRNA genes. Consistent with our previous findings (2, 41), decreased levels of mature snoRNAs are observed in the *pab2*Δ mutant (Fig. 5A, compare lane 3 to lane 1), a consequence of deficient maturation of polyadenylated snoRNA precursors into mature snoRNAs. Strikingly, a significant increase in snoRNA levels was detected in *nab2*Δ cells (Fig. 5A, compare lane 2 to lane 1; see Fig. S3 in the supplemental material for quantifications). These opposite effects on snoRNA expression between *nab2*Δ and *pab2*Δ strains prompted us to analyze the expression of another Pab2-regulated gene, the ribosomal-protein gene *rpl30-2*. Pab2 promotes a nuclear pre-mRNA degradation pathway that competes with RNA splicing to control the expression of selective genes, such as *rpl30-2* (14). In the absence of Pab2, both the mature mRNA and the unspliced pre-mRNA of *rpl30-2* are upregulated (Fig. 5B, lane 3). In contrast, levels of *rpl30-2* mRNA were significantly reduced in the *nab2*Δ mutant (Fig. 5B, lanes 1 and 2, and C). We also found that the levels of unspliced *rpl30-2* pre-mRNA were increased in the *nab2*Δ *pab2*Δ double mutant relative to the *pab2*Δ single mutant (Fig. 5B, compare lane 4 to lane 3, and C), which may reflect the increase in hyperadenylated RNA detected in the double mutant (Fig. 4B). To confirm that the decreased levels of *rpl30-2* mRNA in the *nab2*Δ mutant were specifically due to the absence of Nab2, we tested whether the expression of *nab2* was sufficient to complement this phenotype. Expression of wild-type Nab2 in the *nab2*Δ mutant effectively restored the altered expression of *rpl30-2* (Fig. 5D, compare lanes 2 and 3). In contrast, a variant of Nab2 in which the first cysteine residue of the three zinc finger domains was replaced by alanine did not rescue the decreased levels of *rpl30-2* mRNA in the *nab2*Δ strain (Fig. 5D, lanes 4). These data support opposing roles for Nab2 and Pab2 in gene regulation. Furthermore, given the critical role of the zinc finger motifs of Nab2 in poly(A) binding (Fig. 1E) (19), our results suggest that *S. pombe* Nab2 controls *rpl30-2* expression via poly(A) binding.

Nab2 controls *rpl30-2* expression at the level of unspliced pre-mRNA. To begin to understand how Nab2 and Pab2 play opposite roles in gene regulation, we used *rpl30-2* as a model gene to gain mechanistic insights into how Nab2 functions in gene regulation. Because *nab2*Δ cells show a 2-fold decrease in the steady-state levels of *rpl30-2* mRNA, we first examined the effect of Nab2 deficiency on *rpl30-2* mRNA stability. The drug 1,10-phenanthroline, which is thought to inhibit RNA polymerase II (RNAPII) by sequestering magnesium (43), was used to inhibit transcription of wild-type and *nab2*Δ cells, and RNA decay was followed over time. As a control for transcription inhibition, the level of an unstable transcript, *pma1* (40), rapidly declined after treatment with 1,10-phenanthroline (Fig. 6A and B). As shown in Fig. 6A and B, *rpl30-2* showed similar mRNA stabilities in wild-type and *nab2*Δ cells after transcription inhibition. As the bulk of mRNAs are present in the cytoplasm, mRNA stability assays pri-

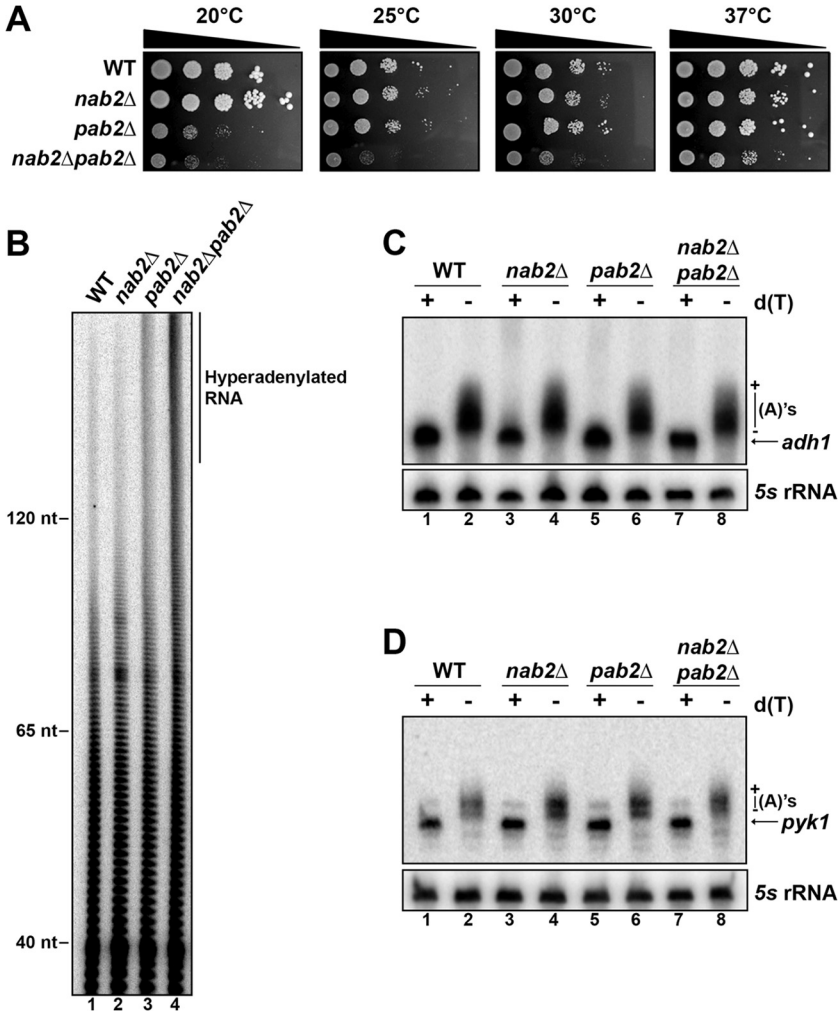

FIG 4 Genetic interaction between Nab2 and Pab2. (A) Tenfold serial dilutions of WT, *nab2*Δ, *pab2*Δ, and *nab2*Δ *pab2*Δ strains. (B) Poly(A) tail length was analyzed by 3′ end labeling of total RNA extracted from the indicated strains, as described in the legend to Fig. 3A. (C and D) Total RNA prepared from wild-type (lanes 1 and 2), *nab2*Δ (lanes 3 and 4), *pab2*Δ (lanes 5 and 6), and *nab2*Δ *pab2*Δ (lanes 7 and 8) cells was treated with RNase H in the presence of DNA oligonucleotides complementary to *adh1* (C) and *pyk1* (D) mRNAs and analyzed as described in the legend to Fig. 3B.

marily measure cytosolic RNA turnover. Accordingly, the similar stabilities of the *rpl30-2* mRNA between wild-type and *nab2*Δ cells, despite a 2-fold reduction in the steady-state level of the *rpl30-2* mRNA in the *nab2*Δ mutant, suggested a nuclear role for Nab2 that is not readily revealed by these stability assays, which primarily examine the turnover of mature cytosolic mRNA. Given the lack of an apparent effect on mRNA stability, we examined whether the decreased levels of *rpl30-2* mRNA observed in the *nab2*Δ mutant could result from reduced transcription. ChIP assays were used to determine the density of RNAPII along the *rpl30-2* gene in wild-type and *nab2*Δ cells. The ChIP experiments showed similar levels of RNAPII along the *rpl30-2* gene in both strains (see Fig. S4 in the supplemental material), indicating no difference in transcription in these mutants. This result suggests that the reduction of *rpl30-2* expression in *nab2*Δ cells is primarily due to regulation at the posttranscriptional level.

To address whether Nab2 directly regulates the expression of *rpl30-2*, RNA coimmunoprecipitation (RIP) experiments were performed to examine whether *rpl30-2* transcripts copurify with Nab2. We therefore purified Nab2-ProA and compared the relative associations with both spliced and unspliced *rpl30-2* transcripts by RT-PCR using a primer across the exon-exon junction for the spliced mRNA and an intron-specific primer for the unspliced pre-mRNA (Fig. 6C). To ensure that the transcripts were posttranscriptional and had undergone polyadenylation, reverse transcription was primed with oligo(dT). Data were normalized to the *nda2* (tubulin) mRNA to control for experimental variation, and values were set to 1.0 for the control purification that was prepared using extracts of an untagged strain. As an additional control, we analyzed immunoprecipitates prepared using a non-RNA-binding protein (Rmt3-ProA), which recovered only low levels of *rpl30-2* transcripts relative to the Nab2-ProA fusion (Fig. 6C). Importantly, we found that the unspliced *rpl30-2* pre-mRNA was ~4-fold more highly associated with Nab2 than the spliced mRNA (Fig. 6C) despite the fact that the unspliced pre-mRNA corresponds to only 5 to 10% of the total *rpl30-2* polyadenylated transcripts (14). These results indicate that a greater proportion of unspliced *rpl30-2* pre-mRNA than spliced mRNA is bound by

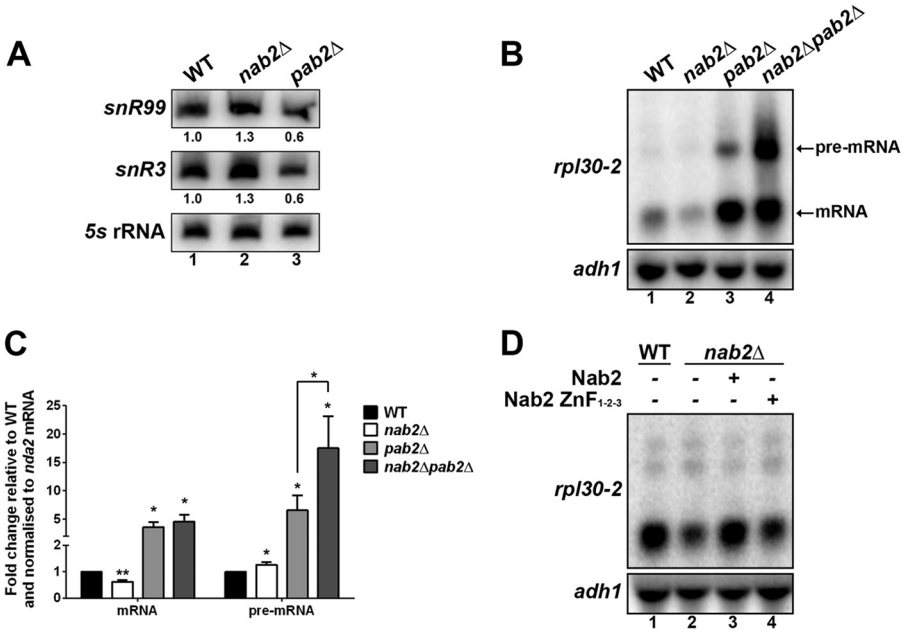

FIG 5 Antagonistic effects of *nab2* and *pab2* deletions. (A) Total RNA prepared from the indicated strains was subjected to Northern blot analysis using probes complementary to the indicated snoRNAs. The 5S rRNA was used as a loading control. The normalized level of each snoRNA relative to wild-type cells is indicated beneath each lane. (B) Northern blot analysis of RNA from the indicated strains. The blot was hybridized using probes specific for *rpl30-2* and *adh1* mRNAs. (C) Quantitative RT-PCR analysis of spliced and unspliced *rpl30-2* RNA levels in the same strains shown in panel B using primer pairs in which one primer spans the exon-exon junction (mRNA) or is complementary to intronic sequences (pre-mRNA). The data and error bars represent the averages and standard deviations from three independent experiments (**, $P < 0.01$; *, $P < 0.05$; Student's *t* test). (D) Northern blot analysis of *rpl30-2* using RNA from wild-type (lane 1) and *nab2*Δ (lanes 2 to 4) cells that were previously transformed with vectors expressing wild-type Nab2 (lane 3), a version of Nab2 with combinatorial cysteine-to-alanine substitutions ($ZnF_{1\text{-}2\text{-}3}$; lane 4), and an empty-vector control (lane 2).

Nab2, suggesting that Nab2 may control *rpl30-2* expression at the level of the unspliced transcript.

To test whether synthesis of the pre-mRNA was required for Nab2-dependent control of *rpl30-2* expression, we used an intronless construct (RPL30-2Δi) that expresses the *rpl30-2* cDNA from native promoter and terminator sequences. As a control, we prepared a similar construct, but using the intron-containing version of *rpl30-2*. These two constructs were chromosomally integrated as a single copy into an *rpl30-2*Δ strain. We then deleted *nab2* from *rpl30-2*Δ strains that expressed intronless and intron-containing versions of *rpl30-2*. As we observed for endogenous *rpl30-2*, expression of the *rpl30-2* intron-containing construct in the *nab2*Δ strain resulted in decreased levels of mRNA relative to the control (Fig. 6D, lanes 1 and 2, and E). In contrast, mRNA levels were not affected in the *nab2*Δ strain when *rpl30-2* was expressed from the intronless construct (Fig. 6D, lanes 3 and 4, and E). These results indicate that Nab2 controls *rpl30-2* expression at the level of the unspliced pre-mRNA.

We previously described a cross-regulatory mechanism between the paralogous ribosomal-protein genes *rpl30-1* and *rpl30-2* in which Rpl30-1 negatively controls *rpl30-2* expression by interfering with RNA splicing, thereby sensitizing the unspliced *rpl30-2* pre-mRNA to nuclear decay via Pab2 and Rrp6 (14). Accordingly, unspliced *rpl30-2* pre-mRNA levels are reduced by 6-fold and spliced mRNA levels increased by ~8-fold in *rpl30-1*Δ cells, as *rpl30-2* splicing was no longer inhibited by Rpl30-1. To test whether Nab2-dependent regulation of *rpl30-2* expression requires splicing interference by Rpl30-1, we compared the levels of *rpl30-2* mRNA between the *rpl30-1*Δ single-mutant strain and the *rpl30-1*Δ *nab2*Δ double mutant. As shown in Fig. 6F, the *rpl30-1*Δ single-mutant strain showed *rpl30-2* mRNA levels similar to those of cells deficient for both *nab2* and *rpl30-1* (compare lanes 3 and 4), suggesting that Nab2 acts downstream of Rpl30-1-dependent splicing inhibition. Altogether, the data presented in Fig. 6 are consistent with a model whereby Nab2 promotes *rpl30-2* expression by targeting the unspliced pre-mRNA.

Nab2 impedes Pab2/Rrp6-dependent pre-mRNA decay. The aforementioned results identify a function for Nab2 as a positive regulator of *rpl30-2* expression via a mechanism that targets the unspliced pre-mRNA. Given that pre-mRNA decay actively competes with splicing during *rpl30-2* expression (14), Nab2 could promote *rpl30-2* expression by interfering with Pab2/Rrp6-mediated pre-mRNA decay or by stimulating RNA splicing. We reasoned that if Nab2 impedes nuclear pre-mRNA decay, levels of *rpl30-2* pre-mRNA should be reduced in *nab2*Δ cells after splicing inhibition, whereas pre-mRNA levels should not change if Nab2 functions as a splicing activator. To distinguish between these possibilities, *nab2* was deleted in two independent strains containing temperature-sensitive mutations in genes (*prp1-4* and *prp2-1*) that encode general splicing factors (44). Total RNA was then prepared from wild-type, *nab2*Δ, *prp1-4*, and *nab2*Δ *prp1-4* double-mutant strains that were grown at the permissive temperature (25°C) or shifted at the nonpermissive temperature of 37°C for 2 h. Almost complete inhibition of pre-mRNA splicing was observed in the *prp1-4* strain after a shift to the nonpermissive temperature, as demonstrated by the accumulation of *rpl30-2* and *tbp1* unspliced pre-mRNAs, together with the concomitant loss of spliced mRNAs (Fig. 7A, compare lane 7 to lane 3). Notably,

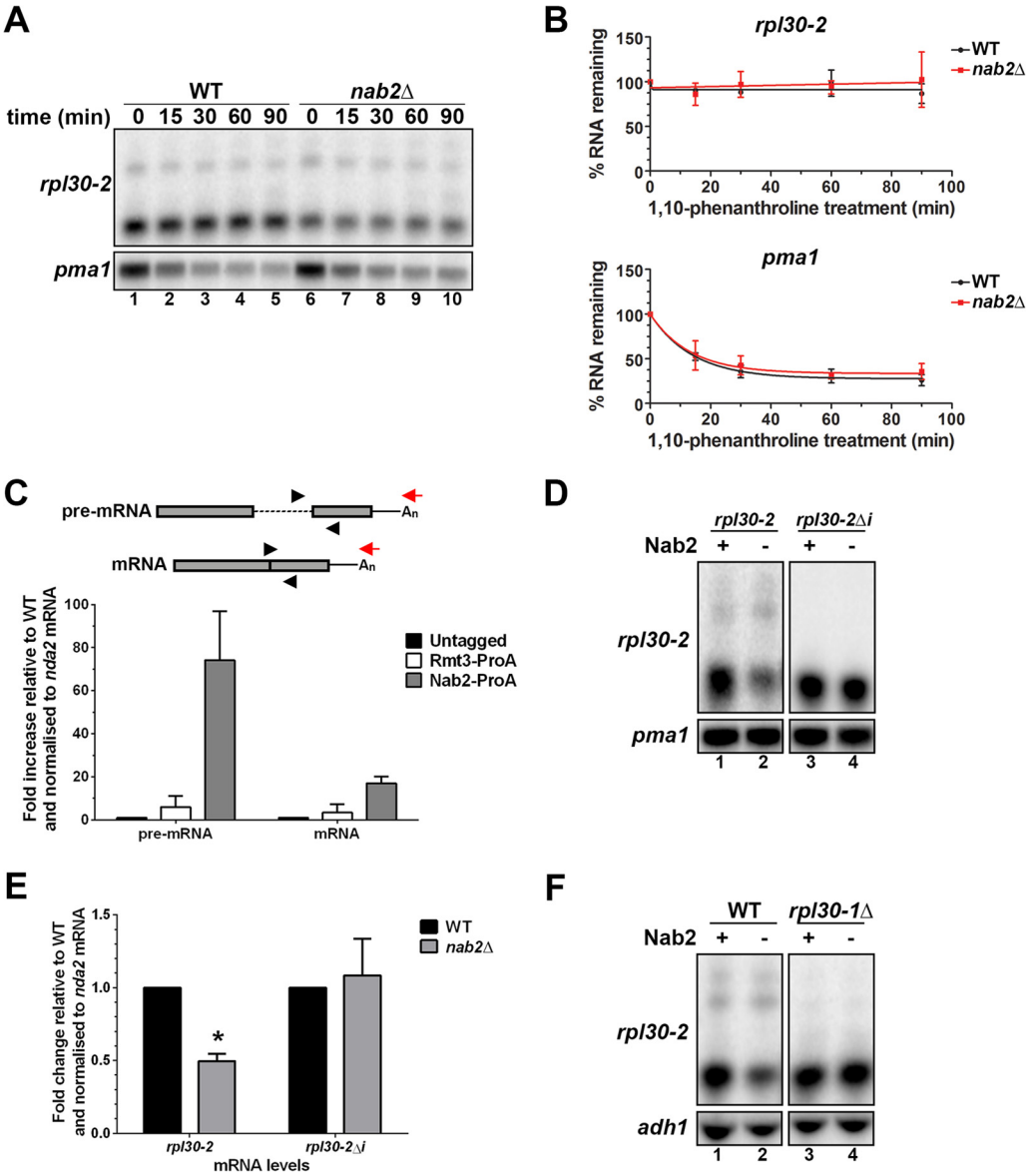

FIG 6 Nab2 promotes *rpl30-2* expression at the level of the unspliced pre-mRNA. (A) Total RNA prepared from wild-type (lanes 1 to 5) and *nab2*Δ (lanes 6 to 10) cells that were previously treated with 1,10-phenanthroline for the indicated times was analyzed by Northern blot analysis for the *rpl30-2* and *pma1* mRNAs. (B) The percentages of RNA remaining for *rpl30-2* (top) and *pma1* (bottom) were determined by quantification of Northern blot data and set to 100% at time zero. The data and error bars represent the averages and standard deviations from three independent experiments. (C) Schematics of primers (arrowheads) used to measure unspliced (upper) and spliced (lower) *rpl30-2* RNA levels after oligo(dT)-mediated reverse transcription (arrows). RIP assays were performed using ProA-tagged versions of Nab2 and Rmt3, as well as an untagged (WT) control strain. Pre-mRNA and mRNA associations (immunoprecipitate/input ratio) were normalized to the *nda2* mRNA. The values were then set to 1.0 for the control purification using the untagged strain. The data and error bars represent the averages and standard deviations from two biological replicates. (D) Northern blot analysis of RNA from wild-type (lanes 1 and 3) and *nab2*Δ (lanes 2 and 4) strains that express *rpl30-2* from intron-containing (lanes 1 and 2) and intronless (RPL30-2Δi; lanes 3 and 4) constructs. (E) Quantitative RT-PCR analysis of *rpl30-2* mRNA levels in the same strains shown in panel D. *, $P < 0.05$; Student's *t* test. (F) Northern analysis of RNA from the indicated strains. The blot was probed for *rpl30-2* and *adh1* mRNAs.

rpl30-2 pre-mRNA levels were reduced in the *nab2*Δ *prp1-4* double mutant relative to the *prp1-4* single-mutant strain (Fig. 7A, top, compare lanes 7 and 8); however, this reduction in pre-mRNA levels was not detected for a Nab2-insensitive control gene (Fig. 7A, *tbp1*). Importantly, the Nab2-dependent reduction in *rpl30-2* pre-mRNA was also observed after the inhibition of RNA splicing using the *prp2-1* splicing mutant (Fig. 7B, compare lanes 7 and 8). As *rpl30-2* transcription levels are not affected by the absence of Nab2 (see Fig. S4 in the supplemental material), these results suggest that Nab2 promotes *rpl30-2* expression upstream of RNA splicing by interfering with pre-mRNA degradation.

The requirement for Nab2 to maintain proper levels of *rpl30-2* pre-mRNA after splicing inhibition suggested that Nab2 might compete with Pab2 to impede the decay of *rpl30-2* pre-mRNAs in the nucleus. If this is the case, excess Nab2 should lead to *rpl30-2* upregulation. To test this idea, we expressed Nab2 from the in-

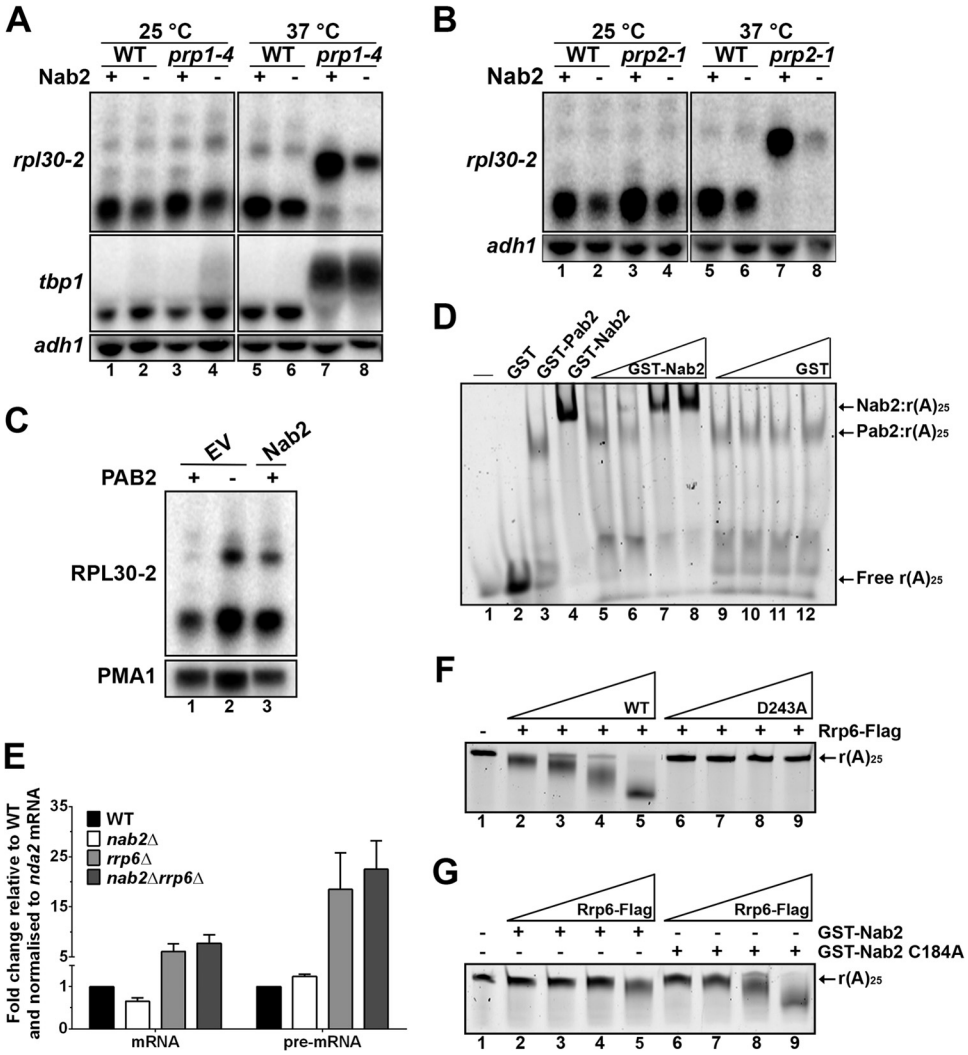

FIG 7 Nab2 interferes with Pab2/Rrp6-mediated decay of unspliced *rpl30-2* pre-mRNA. (A) Total RNA prepared from wild-type (lanes 1 and 5), *nab2*Δ (lanes 2 and 6), *prp1-4* (lanes 3 and 7), and *nab2*Δ *prp1-4* (lanes 4 and 8) strains that were grown at permissive (lanes 1 to 4) and nonpermissive (lanes 5 to 8) temperatures was subjected to Northern blot analysis using probes specific for *rpl30-2*, *tbp1*, and *adh1* transcripts. (B) Total RNA prepared from wild-type (lanes 1 and 5), *nab2*Δ (lanes 2 and 6), *prp2-1* (lanes 3 and 7), and *nab2*Δ *prp2-1* (lanes 4 and 8) strains that were grown at permissive (lanes 1 to 4) and nonpermissive (lanes 5 to 8) temperatures was subjected to Northern blot analysis. (C) Total RNA prepared from wild-type (lanes 1 and 3) and *pab2*Δ (lane 2) cells that were previously transformed with an empty-vector (EV) control (lanes 1 and 2) or a vector expressing Nab2 (lane 3) was subjected to Northern analysis. (D) Equal amounts of GST-Pab2 (lanes 3 and 5 to 12) were incubated with Cy3-r(A)$_{25}$ for 15 min before the addition of increasing amounts of GST-Nab2 (lanes 5 to 8) and GST (lanes 9 to 12) for an additional 15-min incubation. RNA-protein complexes were analyzed as for Fig. 2C. (E) Quantification of Northern blot data for spliced and unspliced *rpl30-2* RNA using the indicated strains. The data and error bars represent the averages and standard deviations from three independent experiments. (F) Increasing amounts of wild-type (lanes 2 to 5) and D243A (lanes 6 to 9) versions of Rrp6 were incubated with Cy3-r(A)$_{25}$ before analysis on a denaturing polyacrylamide gel. (G) Equal amounts of wild-type (lanes 2 to 5) and C184A (lanes 6 to 9) versions of GST-Nab2 were preincubated with Cy3-r(A)$_{25}$ before the addition of increasing amounts of Rrp6 (lanes 2 to 9).

ducible *nmt1*$^+$ promoter, which is induced in the absence of thiamine. In agreement with a direct role of Nab2 in the control of *rpl30-2* expression, excess Nab2 resulted in increased levels of *rpl30-2* mRNA and pre-mRNA relative to cells transformed with a control vector (Fig. 7C, compare lane 3 to lane 1), a phenotype that is similar to that of *pab2*Δ cells (lane 2). Interestingly, we also found that Nab2 can displace Pab2 from poly(A)-bound complexes *in vitro* (Fig. 7D, lanes 5 to 8), whereas GST alone does not (lanes 9 to 12). In contrast, excess Pab2 did not displace previously formed Nab2-poly(A) complexes (see Fig. S5 in the supplemental material). Our data thus suggest that Nab2 and Pab2 promote opposing roles in *rpl30-2* expression by competing for the poly(A) tail of the unspliced *rpl30-2* pre-mRNA.

The exosome-associated exonuclease Rrp6 is the principal degradation factor that promotes the turnover of unspliced *rpl30-2* pre-mRNA in the nucleus (14). Therefore, if Nab2 impedes Rrp6-mediated degradation of *rpl30-2* pre-mRNAs, the absence of Nab2 in the *rrp6*Δ strain is not expected to influence *rpl30-2* mRNA and pre-mRNA levels relative to the *rrp6*Δ single mutant. To test this prediction, we analyzed *rpl30-2* expression levels in wild-type, *nab2*Δ, *rrp6*Δ, and *nab2*Δ *rrp6*Δ double-mutant strains. As shown in Fig. 7E, cells with both *nab2* and *rrp6* deleted showed levels of

rpl30-2 mRNA and pre-mRNA similar to those of the *rrp6*Δ single mutant, consistent with a model in which Nab2 interferes with Rrp6-mediated degradation of *rpl30-2* pre-mRNAs in the nucleus.

To more directly test whether Nab2 can interfere with the 3′→5′ exoribonuclease activity of Rrp6, we purified *S. pombe* Rrp6 from *E. coli* and reconstituted an *in vitro* degradation assay using recombinant Rrp6. Incubation of purified Rrp6 with a poly(A) RNA oligonucleotide [$r(A)_{25}$] labeled with Cy3 at the 5′ end resulted in efficient RNA decay (Fig. 7F, compare lanes 2 to 5 to lane 1). To confirm that this degradation activity was dependent on the exonucleolytic activity of Rrp6, we purified a version of Rrp6 in which an aspartate residue (D243) critical for metal ion coordination in the active site (45, 46) was replaced with alanine. When incubated with the $r(A)_{25}$ substrate RNA, the purified D243A version of *S. pombe* Rrp6 did not degrade poly(A) RNA (Fig. 7F, lanes 6 to 9), indicating that catalytically active Rrp6 is required for poly(A) RNA decay. Importantly, wild-type and D243A versions of Rrp6-Flag showed similar abundances (see Fig. S6 in the supplemental material). We next tested whether Nab2 can interfere with Rrp6-mediated degradation *in vitro*. Wild-type and ZnF-defective versions of GST-Nab2 were incubated with poly(A) RNA before the addition of increasing amounts of wild-type Rrp6. Wild-type Nab2 clearly interfered with the degradation activity of Rrp6 (compare Fig. 7G, lanes 2 to 5, to F, lanes 2 to 5). In contrast, a ZnF-defective version of Nab2 (C184A) that did not bind poly(A) RNA (Fig. 2E) did not impair the exonucleolytic activity of Rrp6 (Fig. 7G, lanes 6 to 9). These data indicate that poly(A)-bound Nab2 can suppress Rrp6-mediated degradation *in vitro*.

DISCUSSION

The addition of a poly(A) tail at the 3′ end of an mRNA is a fundamental step in the course of the gene expression process in eukaryotic cells. However, because the product of polyadenylation corresponds to a widespread and repetitive sequence of adenosines, the poly(A) tail is not generally considered to be involved in gene-specific regulation via *trans*-acting factors. In contrast to this view, we demonstrate here that the 3′ poly(A) tail can function in gene regulation through the action of competing PABPs in the nucleus.

Evolutionarily divergent roles for Nab2 orthologs. Our work describes the identification of the fission yeast ortholog of *S. cerevisiae* Nab2 and human ZC3H14. This conclusion is supported by several observations: (i) the high level of sequence similarity between *S. pombe* Nab2 and its orthologs in the amino- and carboxy-terminal regions (Fig. 1B and C; see Fig. S1 in the supplemental material); (ii) the domain organization of *S. pombe* Nab2, including an N-terminal PWI-like domain and C-terminal CCCH zinc finger motifs (Fig. 1A); (iii) the ability of Nab2 to specifically and directly interact with poly(A) RNA *in vitro* (Fig. 2C to E); and (iv) the nuclear localization of Nab2 (Fig. 2B). Nevertheless, despite sequence and structural homologies, it appears that the function of Nab2 has diverged during the speciation of budding and fission yeasts from a common ancestor. First, in contrast to *S. cerevisiae*, Nab2 is not essential for viability in *S. pombe*. In addition, we did not observe global defects in poly(A) tail length control (Fig. 3A) and in poly(A) RNA export (see Fig. S7 in the supplemental material) in Nab2-deficient *S. pombe* cells, contrasting with what has been reported for loss-of-function alleles of *S. cerevisiae NAB2* (20, 25). Although the reasons for the strikingly different phenotypes related to Nab2 deficiency between budding and fission yeasts are unclear, the presence of an additional nuclear PABP in *S. pombe* (Pab2) may be one explanation. Nab2 is the major nuclear PABP in *S. cerevisiae*, as the genome of *S. cerevisiae* does not encode a homolog of *S. pombe* Pab2/human PABPN1 (47, 48). In contrast, Pab2 is the more abundant nuclear PABP in *S. pombe*, with approximately 5,830 molecules of Pab2 and 2,745 molecules of Nab2 reported per proliferating cell (49). For this reason, *S. pombe* should serve as a powerful model system to gain a detailed understanding of the functional interplay between nuclear PABPs. Accordingly, it will be interesting to define the function of ZC3H14, which shares the human nuclear transcriptome with PABPN1 in a manner analogous to those of *S. pombe* Nab2 and Pab2.

Nuclear PABPs and mRNA polyadenylation. Data obtained from biochemical studies and *in vitro* polyadenylation assays have defined roles for nuclear PABPs in the elongation process of poly(A) polymerase (PAP) and in poly(A) tail length control, suggesting fundamental roles for nuclear PABPs during mRNA polyadenylation *in vivo* (6, 50, 51). In *S. pombe*, however, the current data do not support a role for Pab2 as a general factor required for mRNA polyadenylation. The hyperadenylation phenotype of *pab2*Δ cells affects only a select group of transcripts that accumulate as hyperadenylated RNAs (3, 52, 53), whereas most mRNAs are properly expressed and polyadenylated in *pab2*Δ cells (2). Nevertheless, it was possible that another nuclear PABP, such as Nab2, could stimulate PAP processivity in the absence of Pab2. We were therefore surprised to find that *S. pombe* cells with both *pab2* and *nab2* deleted were viable and produced mRNAs with poly(A) tail lengths similar to those of wild-type cells (Fig. 4C and D). Similarly, Nab2 does not appear to be required to stimulate the elongation process of poly(A) tail synthesis in budding yeast (27). Recent data also indicate that the large majority of human protein-coding genes express normal levels of polyadenylated mRNA in PABPN1-deficient cells (11, 54). These observations question the need for nuclear PABPs to load onto nascent poly(A) tails to stimulate PAP activity during mRNA polyadenylation *in vivo*. Indeed, it may be more efficient in the course of the gene expression process to directly load cytosolic PABPs (Pab1/PABPC1) onto the growing mRNA poly(A) tail before nuclear export, instead of a model in which an exchange reaction must occur between nuclear and cytosolic PABPs to allow efficient cap-dependent translation in the cytoplasm via interactions between the translation initiation complex and PABPC1. Consistent with loading of cytosolic PABPs onto nascent mRNA poly(A) tails in the nucleus, human PABPC1 has been shown to physically associate with unspliced pre-mRNAs (55), as well as to copurify with the mRNA 3′-end processing machinery (56). Functional evidence also supports the critical role of Pab1 in the biogenesis and export of mRNAs in *S. cerevisiae* (27, 57). The development of tools that can determine which PABP is most abundantly loaded onto the nascent poly(A) tail will be an important goal in the future and should provide critical insights into the mechanism underlying control of nuclear mRNA polyadenylation.

Antagonistic roles for nuclear PABPs in gene regulation. Our work shows that whereas the absence of Nab2 does not affect the expression of several housekeeping genes, the expression of Pab2-dependent genes, such as snoRNAs and *rpl30-2*, is affected in *nab2*Δ cells. Specifically, the absence of Nab2 results in converse effects relative to *pab2*Δ cells. Using *rpl30-2* as a model gene, we

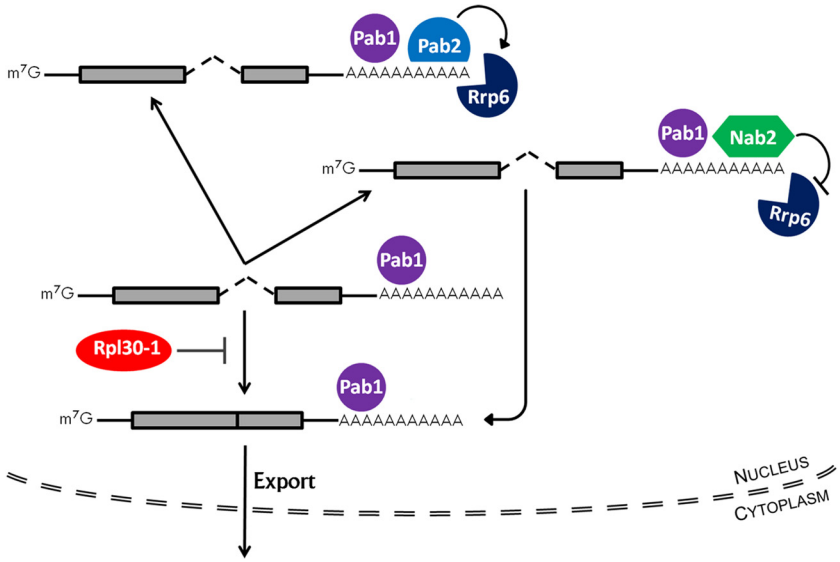

FIG 8 Model for opposing roles of Nab2 and Pab2 in nuclear pre-mRNA decay. Specific RNA binding proteins, such as Rpl30-1, can interfere with RNA splicing, leading to the accumulation of unspliced pre-mRNAs in the nucleus. Pab2-bound pre-mRNAs are targeted for complete degradation via Rrp6-mediated RNA decay, whereas unspliced pre-mRNAs bound by Nab2 are resistant to the degradation activity of Rrp6. Nab2-bound pre-mRNAs can ultimately complete RNA splicing to allow export of mature mRNAs. The equilibrium between RNA decay and processing is therefore influenced by the opposing roles of Pab2 and Nab2, thereby controlling gene expression.

provide evidence that Nab2 preferentially associates with the unspliced pre-mRNA over the mature mRNA. Consistent with this observation, we found that a significant number of splicing factors copurify with Nab2 and that the *rpl30-2* intron is required for Nab2-dependent regulation, indicating that Nab2 acts at the level of the unspliced pre-mRNA. Our data also suggest that Nab2 stabilizes *rpl30-2* pre-mRNAs, as reduced levels of unspliced *rpl30-2* transcripts were found in the absence of Nab2 after splicing inhibition. Based on these findings, we propose that Nab2 controls *rpl30-2* expression by competing with Pab2 for polyadenylated *rpl30-2* pre-mRNAs, thereby interfering with Pab2/Rrp6-mediated pre-mRNA decay in the nucleus (Fig. 8). Consistent with this model, increased dosage of Nab2 in *S. pombe* promotes *rpl30-2* expression by stabilizing the unspliced pre-mRNA, an outcome similar to that of Pab2 deficiency (Fig. 7C). Our findings have therefore unveiled a mechanism of gene regulation in which the 3′ poly(A) tail acts as a platform for competing PABPs in the nucleus. Such a mechanism of gene regulation via antagonistic nuclear PABPs could be controlled by changing the relative Nab2-Pab2 stoichiometry and/or by altering their respective affinities to poly(A) RNA through posttranslational modifications (23, 38, 58, 59).

Given the recently proposed role of *S. cerevisiae* Nab2 in a nuclear surveillance pathway that promotes removal of excess pre-mRNAs via Rrp6 degradation (27), it was surprising to find a role for *S. pombe* Nab2 as a positive regulator of *rpl30-2* expression by a mechanism that impedes nuclear pre-mRNA decay. However, it should be noted that phylogenetic studies indicate that *S. pombe* and *S. cerevisiae* are as different from each other as either is from animals (60). Such evolutionary distance between *S. pombe* and *S. cerevisiae* may explain the different uses of nuclear PABPs in the two species, as discussed above: Pab2 is the major nuclear PABP in *S. pombe*, whereas Pab2 is absent in *S. cerevisiae*. Therefore, although both fission and budding yeasts seem to have conserved a pathway in which pre-mRNA decay competes with RNA splicing to control gene expression, it appears that the large evolutionary distance between the species delegated the RNA decay-promoting function of this pathway to different PABPs: Pab2 in *S. pombe* and Nab2 in *S. cerevisiae* (14, 27). However, we do not exclude the possibility that *S. pombe* Nab2 also contributes to nuclear RNA surveillance, which could explain the additive effect on RNA hyperadenylation noted in the *nab2*Δ *pab2*Δ double mutant relative to the *pab2*Δ single mutant (Fig. 4B).

Our previous work revealed a cross-regulatory mechanism whereby Rpl30-1 negatively controls *rpl30-2* expression via splicing inhibition (14). Importantly, we show here that Nab2-dependent regulation of *rpl30-2* no longer takes place in the absence of Rpl30-1 (Fig. 6F). This finding indicates that the ability of Nab2 to control *rpl30-2* expression at the level pre-mRNA turnover requires that Rpl30-1 interfere with *rpl30-2* splicing beforehand (Fig. 8). As the results indicate that inefficiently spliced transcripts accumulate near their site of transcription (61, 62), we propose that splicing inhibition by a *trans*-acting factor such as Rpl30-1 extends the nuclear lifetime of an unspliced pre-mRNA, allowing nuclear PABPs to compete for pre-mRNA association and regulation (Fig. 8). Gene regulation at the level of nuclear pre-mRNA turnover may therefore provide a means for rapid posttranscriptional control of gene expression in the many cases in which cells must respond quickly to changing environmental conditions (14).

In summary, we provide evidence that the functional interplay between nuclear poly(A)-binding proteins can induce posttranscriptional gene regulation. The opposing roles of Pab2 and Nab2 described in this study imply a need to strictly control the concentration of nuclear PABPs. In this regard, it may be important to consider that diseases related to mutations in *PABPN1*, resulting in oculopharyngeal muscular dystrophy (63), and *ZC3H14*, which cause a form of intellectual disability (29), may be linked to the disruption of this homeostasis.

ACKNOWLEDGMENTS

We thank M. Oeffinger for substantial support with the affinity purifications and F. M. Boisvert for the mass spectrometry analysis.

Funding was provided by Canadian Institutes of Health Research grant MOP219652 to F.B. F.B. is the recipient of a Canada Research Chair.

REFERENCES

1. **LaCava J, Houseley J, Saveanu C, Petfalski E, Thompson E, Jacquier A, Tollervey D.** 2005. RNA degradation by the exosome is promoted by a nuclear polyadenylation complex. Cell **121:**713–724.
2. **Lemay JF, D'Amours A, Lemieux C, Lackner DH, St-Sauveur VG, Bahler J, Bachand F.** 2010. The nuclear poly(A)-binding protein interacts with the exosome to promote synthesis of noncoding small nucleolar RNAs. Mol. Cell **37:**34–45.
3. **St-Andre O, Lemieux C, Perreault A, Lackner DH, Bahler J, Bachand F.** 2010. Negative regulation of meiotic gene expression by the nuclear poly(A)-binding protein in fission yeast. J. Biol. Chem. **285:**27859–27868.
4. **Vanacova S, Wolf J, Martin G, Blank D, Dettwiler S, Friedlein A, Langen H, Keith G, Keller W.** 2005. A new yeast poly(A) polymerase complex involved in RNA quality control. PLoS Biol. **3:**e189. doi:10.1371/journal.pbio.0030189.
5. **Wyers F, Rougemaille M, Badis G, Rousselle JC, Dufour ME, Boulay J, Regnault B, Devaux F, Namane A, Seraphin B, Libri D, Jacquier A.** 2005. Cryptic pol II transcripts are degraded by a nuclear quality control pathway involving a new poly(A) polymerase. Cell **121:**725–737.
6. **Lemay JF, Lemieux C, St-Andre O, Bachand F.** 2010. Crossing the borders: poly(A)-binding proteins working on both sides of the fence. RNA Biol. **7:**291–295.
7. **Kuhn U, Gundel M, Knoth A, Kerwitz Y, Rudel S, Wahle E.** 2009. Poly(A) tail length is controlled by the nuclear poly(A)-binding protein regulating the interaction between poly(A) polymerase and the cleavage and polyadenylation specificity factor. J. Biol. Chem. **284:**22803–22814.
8. **Apponi LH, Leung SW, Williams KR, Valentini SR, Corbett AH, Pavlath GK.** 2010. Loss of nuclear poly(A)-binding protein 1 causes defects in myogenesis and mRNA biogenesis. Hum. Mol. Genet. **19:**1058–1065.
9. **de Klerk E, Venema A, Anvar SY, Goeman JJ, Hu O, Trollet C, Dickson G, den Dunnen JT, van der Maarel SM, Raz V, t'Hoen PA.** 2012. Poly(A) binding protein nuclear 1 levels affect alternative polyadenylation. Nucleic Acids Res. **40:**9089–9101.
10. **Jenal M, Elkon R, Loayza-Puch F, van Haaften G, Kuhn U, Menzies FM, Oude Vrielink JA, Bos AJ, Drost J, Rooijers K, Rubinsztein DC, Agami R.** 2012. The poly(A)-binding protein nuclear 1 suppresses alternative cleavage and polyadenylation sites. Cell **149:**538–553.
11. **Beaulieu YB, Kleinman CL, Landry-Voyer AM, Majewski J, Bachand F.** 2012. Polyadenylation-dependent control of long noncoding RNA expression by the poly(A)-binding protein nuclear 1. PLoS Genet. **8:**e1003078. doi:10.1371/journal.pgen.1003078.
12. **Januszyk K, Lima CD.** 2010. Structural components and architectures of RNA exosomes. Adv. Exp. Med. Biol. **702:**9–28.
13. **Schmid M, Jensen TH.** 2008. The exosome: a multipurpose RNA-decay machine. Trends Biochem. Sci. **33:**501–510.
14. **Lemieux C, Marguerat S, Lafontaine J, Barbezier N, Bahler J, Bachand F.** 2011. A pre-mRNA degradation pathway that selectively targets intron-containing genes requires the nuclear poly(A)-binding protein. Mol. Cell **44:**108–119.
15. **Kuhn U, Wahle E.** 2004. Structure and function of poly(A) binding proteins. Biochim. Biophys. Acta **1678:**67–84.
16. **Mangus DA, Evans MC, Jacobson A.** 2003. Poly(A)-binding proteins: multifunctional scaffolds for the post-transcriptional control of gene expression. Genome Biol. **4:**223.
17. **Kelly SM, Pabit SA, Kitchen CM, Guo P, Marfatia KA, Murphy TJ, Corbett AH, Berland KM.** 2007. Recognition of polyadenosine RNA by zinc finger proteins. Proc. Natl. Acad. Sci. U. S. A. **104:**12306–12311.
18. **Leung SW, Apponi LH, Cornejo OE, Kitchen CM, Valentini SR, Pavlath GK, Dunham CM, Corbett AH.** 2009. Splice variants of the human ZC3H14 gene generate multiple isoforms of a zinc finger polyadenosine RNA binding protein. Gene **439:**71–78.
19. **Brockmann C, Soucek S, Kuhlmann SI, Mills-Lujan K, Kelly SM, Yang JC, Iglesias N, Stutz F, Corbett AH, Neuhaus D, Stewart M.** 2012. Structural basis for polyadenosine-RNA binding by Nab2 Zn fingers and its function in mRNA nuclear export. Structure **20:**1007–1018.
20. **Kelly SM, Leung SW, Apponi LH, Bramley AM, Tran EJ, Chekanova JA, Wente SR, Corbett AH.** 2010. Recognition of polyadenosine RNA by the zinc finger domain of nuclear poly(A) RNA-binding protein 2 (Nab2) is required for correct mRNA 3′-end formation. J. Biol. Chem. **285:**26022–26032.
21. **Soucek S, Corbett AH, Fasken MB.** 2012. The long and the short of it: the role of the zinc finger polyadenosine RNA binding protein, Nab2, in control of poly(A) tail length. Biochim. Biophys. Acta **1819:**546–554.
22. **Iglesias N, Tutucci E, Gwizdek C, Vinciguerra P, Von Dach E, Corbett AH, Dargemont C, Stutz F.** 2010. Ubiquitin-mediated mRNP dynamics and surveillance prior to budding yeast mRNA export. Genes Dev. **24:**1927–1938.
23. **Green DM, Marfatia KA, Crafton EB, Zhang X, Cheng X, Corbett AH.** 2002. Nab2p is required for poly(A) RNA export in Saccharomyces cerevisiae and is regulated by arginine methylation via Hmt1p. J. Biol. Chem. **277:**7752–7760.
24. **Grant RP, Marshall NJ, Yang JC, Fasken MB, Kelly SM, Harreman MT, Neuhaus D, Corbett AH, Stewart M.** 2008. Structure of the N-terminal Mlp1-binding domain of the Saccharomyces cerevisiae mRNA-binding protein, Nab2. J. Mol. Biol. **376:**1048–1059.
25. **Hector RE, Nykamp KR, Dheur S, Anderson JT, Non PJ, Urbinati CR, Wilson SM, Minvielle-Sebastia L, Swanson MS.** 2002. Dual requirement for yeast hnRNP Nab2p in mRNA poly(A) tail length control and nuclear export. EMBO J. **21:**1800–1810.
26. **Batisse J, Batisse C, Budd A, Bottcher B, Hurt E.** 2009. Purification of nuclear poly(A)-binding protein Nab2 reveals association with the yeast transcriptome and a messenger ribonucleoprotein core structure. J. Biol. Chem. **284:**34911–34917.
27. **Schmid M, Poulsen MB, Olszewski P, Pelechano V, Saguez C, Gupta I, Steinmetz LM, Moore C, Jensen TH.** 2012. Rrp6p controls mRNA poly(A) tail length and its decoration with poly(A) binding proteins. Mol. Cell **47:**267–280.
28. **Kelly S, Pak C, Garshasbi M, Kuss A, Corbett AH, Moberg K.** 2012. New kid on the ID block: neural functions of the Nab2/ZC3H14 class of Cys(3)His tandem zinc-finger polyadenosine RNA binding proteins. RNA Biol. **9:**555–562.
29. **Pak C, Garshasbi M, Kahrizi K, Gross C, Apponi LH, Noto JJ, Kelly SM, Leung SW, Tzschach A, Behjati F, Abedini SS, Mohseni M, Jensen LR, Hu H, Huang B, Stahley SN, Liu G, Williams KR, Burdick S, Feng Y, Sanyal S, Bassell GJ, Ropers HH, Najmabadi H, Corbett AH, Moberg KH, Kuss AW.** 2011. Mutation of the conserved polyadenosine RNA binding protein, ZC3H14/dNab2, impairs neural function in Drosophila and humans. Proc. Natl. Acad. Sci. U. S. A. **108:**12390–12395.
30. **Guthrie CR, Schellenberg GD, Kraemer BC.** 2009. SUT-2 potentiates tau-induced neurotoxicity in Caenorhabditis elegans. Hum. Mol. Genet. **18:**1825–1838.
31. **Bahler J, Wu JQ, Longtine MS, Shah NG, McKenzie A, III, Steever AB, Wach A, Philippsen P, Pringle JR.** 1998. Heterologous modules for efficient and versatile PCR-based gene targeting in Schizosaccharomyces pombe. Yeast **14:**943–951.
32. **Arnold K, Bordoli L, Kopp J, Schwede T.** 2006. The SWISS-MODEL workspace: a web-based environment for protein structure homology modelling. Bioinformatics **22:**195–201.
33. **Brunger AT.** 2007. Version 1.2 of the Crystallography and NMR system. Nat. Protoc. **2:**2728–2733.
34. **Emsley P, Cowtan K.** 2004. Coot: model-building tools for molecular graphics. Acta Crystallogr. D Biol. Crystallogr. **60:**2126–2132.
35. **Beaudoin J, Labbe S.** 2006. Copper induces cytoplasmic retention of fission yeast transcription factor cuf1. Eukaryot. Cell **5:**277–292.
36. **Craven RA, Griffiths DJ, Sheldrick KS, Randall RE, Hagan IM, Carr AM.** 1998. Vectors for the expression of tagged proteins in Schizosaccharomyces pombe. Gene **221:**59–68.
37. **Mallet PL, Bachand F.** 2013. A proline-tyrosine nuclear localization signal (PY-NLS) is required for the nuclear import of fission yeast PAB2, but not of human PABPN1. Traffic **14:**282–294.
38. **Perreault A, Lemieux C, Bachand F.** 2007. Regulation of the nuclear poly(A)-binding protein by arginine methylation in fission yeast. J. Biol. Chem. **282:**7552–7562.
39. **Oeffinger M.** 2012. Two steps forward—one step back: advances in affinity purification mass spectrometry of macromolecular complexes. Proteomics **12:**1591–1608.
40. **Lackner DH, Beilharz TH, Marguerat S, Mata J, Watt S, Schubert F,**

Preiss T, Bahler J. 2007. A network of multiple regulatory layers shapes gene expression in fission yeast. Mol. Cell **26:**145–155.
41. **Larochelle M, Lemay JF, Bachand F.** 2012. The THO complex cooperates with the nuclear RNA surveillance machinery to control small nucleolar RNA expression. Nucleic Acids Res. **40:**10240–10253.
42. **Berriz GF, King OD, Bryant B, Sander C, Roth FP.** 2003. Characterizing gene sets with FuncAssociate. Bioinformatics **19:**2502–2504.
43. **Grigull J, Mnaimneh S, Pootoolal J, Robinson MD, Hughes TR.** 2004. Genome-wide analysis of mRNA stability using transcription inhibitors and microarrays reveals posttranscriptional control of ribosome biogenesis factors. Mol. Cell. Biol. **24:**5534–5547.
44. **Habara Y, Urushiyama S, Shibuya T, Ohshima Y, Tani T.** 2001. Mutation in the prp12+ gene encoding a homolog of SAP130/SF3b130 causes differential inhibition of pre-mRNA splicing and arrest of cell-cycle progression in Schizosaccharomyces pombe. RNA **7:**671–681.
45. **Midtgaard SF, Assenholt J, Jonstrup AT, Van LB, Jensen TH, Brodersen DE.** 2006. Structure of the nuclear exosome component Rrp6p reveals an interplay between the active site and the HRDC domain. Proc. Natl. Acad. Sci. U. S. A. **103:**11898–11903.
46. **Phillips S, Butler JS.** 2003. Contribution of domain structure to the RNA 3′ end processing and degradation functions of the nuclear exosome subunit Rrp6p. RNA **9:**1098–1107.
47. **Banerjee A, Apponi LH, Pavlath GK, Corbett AH.** 2013. PABPN1: molecular function and muscle disease. FEBS J. **280:**4230–4250.
48. **Winstall E, Sadowski M, Kuhn U, Wahle E, Sachs AB.** 2000. The Saccharomyces cerevisiae RNA-binding protein Rbp29 functions in cytoplasmic mRNA metabolism. J. Biol. Chem. **275:**21817–21826.
49. **Marguerat S, Schmidt A, Codlin S, Chen W, Aebersold R, Bahler J.** 2012. Quantitative analysis of fission yeast transcriptomes and proteomes in proliferating and quiescent cells. Cell **151:**671–683.
50. **Eckmann CR, Rammelt C, Wahle E.** 2011. Control of poly(A) tail length. Wiley Interdiscip. Rev. RNA **2:**348–361.
51. **Viphakone N, Voisinet-Hakil F, Minvielle-Sebastia L.** 2008. Molecular dissection of mRNA poly(A) tail length control in yeast. Nucleic Acids Res. **36:**2418–2433.
52. **Chen HM, Futcher B, Leatherwood J.** 2011. The fission yeast RNA binding protein Mmi1 regulates meiotic genes by controlling intron specific splicing and polyadenylation coupled RNA turnover. PLoS One **6:**e26804. doi:10.1371/journal.pone.0026804.
53. **Yamanaka S, Yamashita A, Harigaya Y, Iwata R, Yamamoto M.** 2010. Importance of polyadenylation in the selective elimination of meiotic mRNAs in growing S. pombe cells. EMBO J. **29:**2173–2181.
54. **Bhattacharjee RB, Bag J.** 2012. Depletion of nuclear poly(A) binding protein PABPN1 produces a compensatory response by cytoplasmic PABP4 and PABP5 in cultured human cells. PLoS One **7:**e53036. doi:10.1371/journal.pone.0053036.
55. **Hosoda N, Lejeune F, Maquat LE.** 2006. Evidence that poly(A) binding protein C1 binds nuclear pre-mRNA poly(A) tails. Mol. Cell. Biol. **26:**3085–3097.
56. **Shi Y, Di Giammartino DC, Taylor D, Sarkeshik A, Rice WJ, Yates JR, III, Frank J, Manley JL.** 2009. Molecular architecture of the human pre-mRNA 3′ processing complex. Mol. Cell **33:**365–376.
57. **Dunn EF, Hammell CM, Hodge CA, Cole CN.** 2005. Yeast poly(A)-binding protein, Pab1, and PAN, a poly(A) nuclease complex recruited by Pab1, connect mRNA biogenesis to export. Genes Dev. **19:**90–103.
58. **Le H, Browning KS, Gallie DR.** 2000. The phosphorylation state of poly(A)-binding protein specifies its binding to poly(A) RNA and its interaction with eukaryotic initiation factor (eIF) 4F, eIFiso4F, and eIF4B. J. Biol. Chem. **275:**17452–17462.
59. **Lee J, Bedford MT.** 2002. PABP1 identified as an arginine methyltransferase substrate using high-density protein arrays. EMBO Rep. **3:**268–273.
60. **Sipiczki M.** 2000. Where does fission yeast sit on the tree of life? Genome Biol. **1:**REVIEWS1011. doi:10.1186/gb-2000-1-2-reviews1011.
61. **de Almeida SF, Garcia-Sacristan A, Custodio N, Carmo-Fonseca M.** 2010. A link between nuclear RNA surveillance, the human exosome and RNA polymerase II transcriptional termination. Nucleic Acids Res. **38:**8015–8026.
62. **Eberle AB, Hessle V, Helbig R, Dantoft W, Gimber N, Visa N.** 2010. Splice-site mutations cause Rrp6-mediated nuclear retention of the unspliced RNAs and transcriptional down-regulation of the splicing-defective genes. PLoS One **5:**e11540. doi:10.1371/journal.pone.0011540.
63. **Brais B, Bouchard JP, Xie YG, Rochefort DL, Chretien N, Tome FM, Lafreniere RG, Rommens JM, Uyama E, Nohira O, Blumen S, Korczyn AD, Heutink P, Mathieu J, Duranceau A, Codere F, Fardeau M, Rouleau GA.** 1998. Short GCG expansions in the PABP2 gene cause oculopharyngeal muscular dystrophy. Nat. Genet. **18:**164–167.